

AD-A061 084 NAVAL UNDERWATER SYSTEMS CENTER NEW LONDON CONN NEW --ETC F/G 20/14
QUASI-STATIC RANGE PROPAGATION EQUATIONS FOR THE APPROXIMATE FI--ETC(U)
OCT 78 P R BANNISTER, R L DUBE
UNCLASSIFIED NUSC-TR-5807 NL

1 of 1
AD
A061 084

END
DATE
FILMED
1-79
DDC

ADA061084

NUSC Technical Report 5807

DDC FILE COPY

LEVEL II

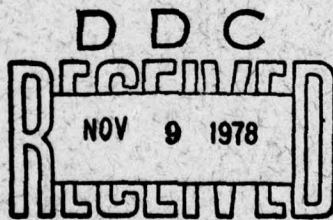
NUSC Technical Report 5807

Handwritten signature/initials
B.S.



Quasi-Static Range Propagation Equations For the Approximate Fields Within a Conducting Slab

**Peter R. Bannister
René L. Dube
Submarine Electromagnetic
Systems Department**



2 October 1978

NUSC

**NAVAL UNDERWATER SYSTEMS CENTER
Newport, Rhode Island • New London, Connecticut**

Approved for public release; distribution unlimited.

78 10 27 082

PREFACE

This report was prepared under NUSC Project No. A-532-24, Principal Investigator, P. R. Bannister (Code 341). Naval Industrial funding was received from the David W. Taylor Naval Ship Research and Development Center, W. J. Andahazy, Project Director. The sponsor was the Naval Sea Systems Command, Project Program Manager, W. L. Welsh (SEA-03424).

The Technical Reviewer for this report was J. Tennyson (Code 3403).

REVIEWED AND APPROVED: 2 October 1978

for J. Dence
John Merrill
**Head: Submarine Electromagnetic
Systems Department**

The authors of this report are located at the New London
Laboratory, Naval Underwater Systems Center,
New London, Connecticut 06320

19. (Cont'd)

Quasi-Near Range
Quasi-Static Range
Quasi-Static Range Subsurface-to-Subsurface Propagation
Vertical Electric Dipole (VED)
Vertical Magnetic Dipole (VMD)

LEVEL II

ADMISSION to	
DTIC	White Section <input checked="" type="checkbox"/>
DDC	Soft Section <input type="checkbox"/>
UNANNOUNCED	<input type="checkbox"/>
JUSTIFICATION.....	
BY.....	
DISTRIBUTION/AVAILABILITY CODE	
Dist.	AVAIL. and/or SPECIAL
A	

DDC
RECEIVED
NOV 9 1978
RECEIVED
D

TABLE OF CONTENTS

	Page
LIST OF ILLUSTRATIONS.	11
INTRODUCTION	1
MODIFIED FINITELY-CONDUCTING, EARTH-IMAGE THEORY TECHNIQUES. .	2
DERIVATION OF THE CONDUCTING SLAB FIELD-COMPONENT EXPRESSIONS FOR THE GENERAL QUASI-STATIC RANGE	3
Horizontal Electric Dipole (HED).	4
Horizontal Magnetic Dipole (HMD).	6
Vertical Electric Dipole (VED).	7
Vertical Magnetic Dipole (VMD).	8
DERIVATION OF THE CONDUCTING SLAB FIELD-COMPONENT EXPRESSIONS FOR THE QUASI-NEAR RANGE	9
Long Horizontal Line Source/Antenna	9
Horizontal Electric Dipole (HED) Antenna.	12
Horizontal Magnetic Dipole (HMD) Antenna.	13
Vertical Magnetic Dipole (VMD) Antenna.	13
DISCUSSION	14
CONCLUSIONS.	15
REFERENCES	23

LIST OF ILLUSTRATIONS

Figure		Page
1	Conducting Slab Geometry.	17
2	Comparison of Modified Image Theory, Asymptotic Theory, and Weaver's Result for the $E\beta$ Component	18
3	Comparison of Modified Image Theory, Asymptotic Theory, and Weaver's Result for the $E\phi$ Component	19
4	Comparison of Modified Image Theory, Asymptotic Theory, and Weaver's Result for the $H\beta$ Component	20
5	Comparison of Modified Image Theory, Asymptotic Theory, and Weaver's Result for the $H\phi$ Component	21
6	Comparison of Modified Image Theory, Asymptotic Theory, and Weaver's Result for the H_z^2 Component	21

QUASI-STATIC RANGE PROPAGATION EQUATIONS
FOR THE APPROXIMATE FIELDS WITHIN
A CONDUCTING SLAB

INTRODUCTION

During the last several years, considerable interest has developed in determining the quasi-static field components of antennas located above, or buried within, the earth's surface. Quasi-static range is defined as the range of transmission where the measurement distance is much less than a free-space wavelength. Quasi-static range results are useful for submarine radio communication and detection; they also have applications in locating buried miners and help geophysicists determine the electrical properties of the earth.

For the semi-infinite conducting medium case (i.e., air, single layered earth), some work has been done to determine the quasi-static fields produced by various subsurface sources when the measurement distance is comparable to the earth skin depth.¹⁻⁶ (Most of these results are summarized by Kraichman.⁷) However, the field strength expressions are very complex because they involve products of modified Bessel functions of different argument. Recently, by using finitely conducting earth-image theory techniques, we derived approximate expressions for the general quasi-static range electromagnetic fields (in air and in earth) produced by various subsurface antennas.⁸ Some numerical calculations have also been provided.⁹

These investigations revealed that when the source is not buried too far from the surface of the conducting half-space, the resultant electromagnetic field is significantly different from that obtained in an infinite conducting medium. Therefore, if the conductor is two-layered, the lower interface must likewise affect the field (especially if the upper layer in which the source is located is not too deep). For example, if the transmitting antenna is situated in a shallow sea, the theory for a uniform conducting half-space would not accurately describe the field at the sea bottom. This observation is also true at the surface of the sea if the sea depth (l_1) is less than approximately one skin depth.

Weaver has evaluated the exact Sommerfeld integral expressions and obtained numerical results for the quasi-static fields produced by horizontal and vertical electric dipole (HED and VED) antennas located in the upper layer of a two-layer conducting half-space.⁶ Numerical results for the quasi-static fields produced in the sea by a vertical magnetic dipole (VMD) for various values of sea bottom conductivity have been obtained by Coggon and Morrison.¹⁰

This report employs finitely conducting earth-image theory techniques to derive approximate expressions for the general ac quasi-static range electromagnetic fields produced by various subsurface dipole antennas, which include the HED, VED, VMD, and horizontal magnetic dipole (HMD) types, each of which is located in the upper layer of a two-layer conducting earth. For mathematical convenience, consider the conductivity of the bottom layer as being equal to zero. Thus, the problem is reduced to calculating the fields in a conducting slab. Treating the bottom layer conductivity as equal to zero is not

that restrictive; in many practical cases, the conductivity of the upper layer (σ_1) is much greater than the conductivity of the bottom layer (σ_2), particularly in the sea-to-sea bed case. Therefore, this assumption limits the results to measurement distances (ρ) of approximately $\delta_2/5$, where δ_2 is the skin depth in the bottom layer. For example, at a frequency of 1 Hz, if $\sigma_1 = 4$ S/m (sea) and $\sigma_2 = 10^{-2}$ S/m (sea bed), then $\delta_1 \sim 250$ m and $\delta_2 \sim 5$ km. Therefore, for this example, the results should be valid to a measurement distance of approximately 1 km. Furthermore, if the conductivity of the sea bed is 10^{-4} S/m ($\delta_2 \sim 50$ km), the results should be valid to a measurement distance of approximately 10 km.

For the purpose of this report, all four sources are located at depth h ($h \geq 0$) with respect to a cylindrical coordinate system (ρ, ϕ, z) and are assumed to carry a constant current, I . The VED and HED antennas (of infinitesimal length ℓ) are oriented in the z and x directions, respectively. The axes of the VMD and HMD antennas (of infinitesimal area A) are oriented in the z and y directions, respectively. Free space occupies the regions $z < 0$ and $z > \ell_1$, whereas the conducting slab occupies the region $0 < z < \ell_1$ (see figure 1).^{*} Displacement currents are neglected in both the slab and the air. The magnetic permeability of the conducting slab is assumed to equal μ_0 , the permeability of free space. Meter-kilogram-second (mks) units are employed and a suppressed time factor of $\exp(i\omega t)$ is assumed.

MODIFIED FINITELY-CONDUCTING, EARTH-IMAGE THEORY TECHNIQUES

In the semi-infinite conducting medium, where both the source and receiving antennas are located above the earth's surface ($z, h < 0$) (see figure 1), the quasi-static range ($\gamma_0 \sim 0$) integrals are of the type that can not be evaluated analytically throughout the quasi-static range,¹¹ that is

$$I_1 \sim \int_0^{\infty} \left(\frac{u - \lambda}{u + \lambda} \right) e^{\lambda(z+h)} J_0(\lambda\rho) d\lambda, \quad (1)$$

where

$$\gamma_0 = i\omega(\mu_0\epsilon_0)^{1/2} \sim 0 \text{ (air),}$$

$$\gamma \sim (i\omega\mu_0\sigma)^{1/2} \text{ (earth),}$$

$$u = (\lambda^2 + \gamma^2)^{1/2}, \text{ and}$$

$J_0(\lambda\rho)$ = Bessel function of the first kind, order zero, and argument $\lambda\rho$.

^{*}Figures 1 through 6 are presented at the end of the text.

Physically, the essence of the finitely conducting earth-image theory technique is to replace the finitely conducting earth with a perfectly conducting earth located at the (complex) depth $d/2$, where $d = 2/\gamma = \delta(1-i)$. Analytically, this corresponds to replacing the algebraic reflection coefficient $(u-\lambda)/(u+\lambda)$ in the exact integral equations by $\exp(-\lambda d)$, where λ is the variable of integration. Once this is accomplished, (1) can be readily evaluated. For antennas located at, or above, the earth's surface, the general image theory approximation is valid throughout the quasi-static range.^{11,12}

When the source and receiving antennas are located below the earth's surface ($z, h > 0$) (see figure 1), the quasi-static range integrals to be evaluated are of the form^{1-6,8}

$$I_2 \sim \int_0^{\infty} \left(\frac{u-\lambda}{u+\lambda} \right) e^{-u(z+h)} J_0(\lambda \rho) d\lambda \quad (2)$$

Integrals of this type can, and have, been evaluated analytically throughout the quasi-static range.¹⁻⁶ However, the resulting expressions are very complex because they involve products of modified Bessel functions of different argument. Therefore, we let⁸

$$e^{-u(z+h)} \sim e^{-\gamma a(z+h)} e^{-\gamma b(z+h)}, \quad (3)$$

where

$$a = 0 \text{ and } b = 1 \text{ for } R_1/\delta \ll 1 \left[R_1 = \sqrt{\rho^2 + (z+h)^2} \right],$$

$$a = 0.4 \text{ and } b = 0.96 \text{ for } R_1/\delta \text{ less than approximately } 1,$$

$$a = 0.96 \text{ and } b = 0.4 \text{ for } R_1/\delta \text{ between approximately } 1 \text{ and } 10, \text{ and}$$

$$a = 1 \text{ and } b = 0 \text{ for } \rho > 3(z+h).$$

Substituting (3) into (2) and substituting $\exp(-\lambda d)$ for $(u-\lambda)/(u+\lambda)$ results in

$$I_2 \sim e^{-\gamma a(z+h)} \int_0^{\infty} e^{-\lambda [d + b(z+h)]} J_0(\lambda \rho) d\lambda, \quad (4)$$

which can be readily evaluated throughout the quasi-static range.

DERIVATION OF THE CONDUCTING SLAB FIELD-COMPONENT EXPRESSIONS FOR THE GENERAL QUASI-STATIC RANGE

Because we have already derived the general quasi-static range sub-surface-to-subsurface field-component expressions for the semi-infinite

medium case, we can employ these results and the method of images to derive approximate expressions for the ac quasi-static fields within a conducting slab.⁸ In this situation, the multiple image pattern is an infinite array that supplements the original dipole exactly as the images of a physical object located between two plane mirrors appear to be an infinite array of that object.

HORIZONTAL ELECTRIC DIPOLE (HED)

The HED equations can easily be derived from equations (64) through (69) of an earlier report.⁸ They are

$$E_{\rho} \sim \frac{I l \cos \phi}{4\pi\sigma} \sum_{n=0}^{\infty} \epsilon_n \left\{ \frac{e^{-\gamma R_{ON}}}{R_{ON}^3} \left[\left(\frac{3\rho^2}{R_{ON}^2} - 1 \right) (1 + \gamma R_{ON}) - \gamma^2 X_1^2 \right] \right. \\ \left. - \frac{e^{-\gamma R_{IN}}}{R_{IN}^3} \left[\left(\frac{3\rho^2}{R_{IN}^2} - 1 \right) (1 + \gamma R_{IN}) - \gamma^2 X_2^2 \right] \right. \\ \left. + \frac{2e^{-\gamma a X_2}}{A_{1N}^3} \left[1 + b - \frac{3b^3 X_2^2}{A_{1N}^2} - \gamma a b X_2 \right] \right\}, \quad (5)$$

$$E_{\phi} \sim \frac{I l \sin \phi}{4\pi\sigma} \sum_{n=0}^{\infty} \epsilon_n \left\{ \frac{e^{-\gamma R_{ON}}}{R_{ON}^3} \left[1 + \gamma R_{ON} + \gamma^2 R_{ON}^2 \right] \right. \\ \left. - \frac{e^{-\gamma R_{IN}}}{R_{IN}^3} \left[1 + \gamma R_{IN} + \gamma^2 R_{IN}^2 \right] \right. \\ \left. + \frac{2e^{-\gamma a X_2}}{A_{1N}^3} \left[1 + \frac{2A_{1N}^2}{d^2} \left(1 - \frac{A_{1N}}{A_{2N}} \right) \right] \right\}, \quad (6)$$

$$E_z \sim \frac{I l \cos \phi}{4\pi\sigma} \sum_{n=0}^{\infty} \rho \epsilon_n \left[\frac{X_1}{R_{ON}^5} \left(3 + 3\gamma R_{ON} + \gamma^2 R_{ON}^2 \right) e^{-\gamma R_{ON}} \right. \\ \left. + \frac{X_2}{R_{IN}^5} \left(3 + 3\gamma R_{IN} + \gamma^2 R_{IN}^2 \right) e^{-\gamma R_{IN}} \right], \quad (7)$$

$$H_{\rho} \sim -\frac{I\ell \sin \phi}{4\pi} \sum_{n=0}^{\infty} \epsilon_n \left\{ \left[\frac{d + bX_2}{\rho^2 A_{2N}} - \frac{bX_2}{\rho^2 A_{1N}} \right] e^{-\gamma a X_2} \right. \\ \left. + \frac{X_1}{3 R_{ON}} (1 + \gamma R_{ON}) e^{-\gamma R_{ON}} + \frac{(d + bX_2)}{3 A_{2N}} e^{-\gamma a X_2} \right\}, \quad (8)$$

$$H_{\phi} \sim -\frac{I\ell \cos \phi}{4\pi} \sum_{n=0}^{\infty} \epsilon_n \left\{ \frac{X_1}{3 R_{ON}} (1 + \gamma R_{ON}) e^{-\gamma R_{ON}} \right. \\ \left. + \frac{X_2}{3 R_{1N}} (1 + \gamma R_{1N}) e^{-\gamma R_{1N}} - \frac{e^{-\gamma a X_2}}{\rho^2} \left[\frac{d + bX_2}{A_{2N}} - \frac{bX_2}{A_{1N}} \right] \right\}, \quad (9)$$

$$H_z \sim \frac{I\ell \sin \phi}{4\pi} \sum_{n=0}^{\infty} \rho \epsilon_n \left\{ \frac{e^{-\gamma R_{ON}}}{3 R_{ON}} (1 + \gamma R_{ON}) - \frac{e^{-\gamma R_{1N}}}{3 R_{1N}} (1 + \gamma R_{1N}) \right. \\ \left. + e^{-\gamma a X_2} \left[\frac{1}{3 A_{1N}} - \frac{1}{3 A_{2N}} \right] \right\}, \quad (10)$$

where

$$X_1 = 2n\ell_1 + z - h,$$

$$X_2 = 2n\ell_1 + z + h,$$

$$R_{ON}^2 = \rho^2 + X_1^2,$$

$$R_{1N}^2 = \rho^2 + X_2^2,$$

$$A_{1N}^2 = \rho^2 + b^2 X_2^2,$$

$$A_{2N}^2 = \rho^2 + (d + bX_2)^2, \text{ and}$$

$$\epsilon_0 = 1, \epsilon_n = 2, n = 1, 2, 3, \dots$$

HORIZONTAL MAGNETIC DIPOLE (HMD)

The HMD equations can be derived from equations (76) through (81) of an earlier report.⁸ They are

$$E_\rho \sim -\frac{i\omega\mu_0 IA \cos\phi}{4\pi} \sum_{n=0}^{\infty} \epsilon_n \left\{ \frac{X_1}{R_{ON}^3} (1 + \gamma R_{ON}) e^{-\gamma R_{ON}} \right. \\ \left. - \frac{X_2}{R_{IN}^2} (1 + \gamma R_{IN}) e^{-\gamma R_{IN}} + \frac{e^{-\gamma a X_2}}{\rho^2} \left[\frac{d + bX_2}{A_{2N}} - \frac{bX_2}{A_{1N}} \right] \right\}, \quad (11)$$

$$E_\phi \sim -\frac{i\omega\mu_0 IA \sin\phi}{4\pi} \sum_{n=0}^{\infty} \epsilon_n \left\{ -\frac{X_1}{R_{ON}^3} (1 + \gamma R_{ON}) e^{-\gamma R_{ON}} \right. \\ \left. + \frac{(d + bX_2)}{A_{2N}^3} e^{-\gamma a X_2} + \frac{e^{-\gamma a X_2}}{\rho^2} \left[\frac{d + bX_2}{A_{2N}} - \frac{bX_2}{A_{1N}} \right] \right\}, \quad (12)$$

$$E_z \sim \frac{i\omega\mu_0 IA \cos\phi}{4\pi} \sum_{n=0}^{\infty} \rho \epsilon_n \left[\frac{e^{-\gamma R_{ON}}}{R_{ON}^3} (1 + \gamma R_{ON}) \right. \\ \left. - \frac{e^{-\gamma R_{IN}}}{R_{IN}^3} (1 + \gamma R_{IN}) \right], \quad (13)$$

$$\begin{aligned}
 H_{\rho} \sim & \frac{IA \sin \phi}{4\pi} \sum_{n=0}^{\infty} \epsilon_n \left\{ \frac{e^{-\gamma R_{ON}}}{R_{ON}^3} \left[\left(1 - \frac{3\rho^2}{R_{ON}^2} \right) (1 + \gamma R_{ON}) + \gamma^2 X_1^2 \right] \right. \\
 & - \frac{e^{-\gamma R_{1N}}}{R_{1N}^3} \left[\left(1 - \frac{3\rho^2}{R_{1N}^2} \right) (1 + \gamma R_{1N}) + \gamma^2 X_2^2 \right] \\
 & \left. + e^{-\gamma a X_2} \left[\frac{1}{A_{1N}^3} \left(1 - \frac{3\rho^2}{A_{1N}^2} \right) + \frac{1}{A_{2N}^3} \left(1 - \frac{3\rho^2}{A_{2N}^2} \right) \right] \right\}, \quad (14)
 \end{aligned}$$

$$\begin{aligned}
 H_{\phi} \sim & \frac{IA \cos \phi}{4\pi} \sum_{n=0}^{\infty} \epsilon_n \left[\frac{e^{-\gamma R_{ON}}}{R_{ON}^3} (1 + \gamma R_{ON} + \gamma^2 R_{ON}^2) \right. \\
 & \left. - \frac{e^{-\gamma R_{1N}}}{R_{1N}^3} (1 + \gamma R_{1N} + \gamma^2 R_{1N}^2) + e^{-\gamma a X_2} \left(\frac{1}{A_{1N}^3} + \frac{1}{A_{2N}^3} \right) \right], \quad (15)
 \end{aligned}$$

and

$$\begin{aligned}
 H_z \sim & \frac{IA \sin \phi}{4\pi} \sum_{n=0}^{\infty} \rho \epsilon_n \left[-\frac{X_1}{R_{ON}^5} (3 + 3\gamma R_{ON} + \gamma^2 R_{ON}^2) e^{-\gamma R_{ON}} \right. \\
 & \left. + \frac{3(d + bX_2)}{A_{2N}^5} e^{-\gamma a X_2} \right]. \quad (16)
 \end{aligned}$$

VERTICAL ELECTRIC DIPOLE (VED)

The VED equations can be derived from equations (73) through (75) of an earlier report.⁸ They are

$$E_{\rho} \sim \frac{I l}{4\pi \sigma} \sum_{n=0}^{\infty} \rho \epsilon_n \left[\frac{X_1}{R_{ON}^5} (3 + 3\gamma R_{ON} + \gamma^2 R_{ON}^2) e^{-\gamma R_{ON}} \right.$$

$$- \frac{X_2}{R_{1N}^5} \left(3 + 3Y_{R_{1N}} + Y_{R_{1N}}^2 \right) e^{-Y_{R_{1N}}} \Bigg], \quad (17)$$

$$E_z \sim - \frac{I\ell}{4\pi\sigma} \sum_{n=0}^{\infty} \epsilon_n \left\{ \frac{e^{-Y_{R_{ON}}}}{R_{ON}^3} \left[\left(1 - \frac{3X_1^2}{R_{ON}^2} \right) \left(1 + Y_{R_{ON}} \right) + Y_{R_{ON}}^2 \right] \right. \\ \left. - \frac{e^{-Y_{R_{1N}}}}{R_{1N}^3} \left[\left(1 - \frac{3X_2^2}{R_{1N}^2} \right) \left(1 + Y_{R_{1N}} \right) + Y_{R_{1N}}^2 \right] \right\}, \quad (18)$$

and

$$H_\phi \sim \frac{I\ell}{4\pi} \sum_{n=0}^{\infty} \rho \epsilon_n \left[\frac{e^{-Y_{R_{ON}}}}{R_{ON}^3} \left(1 + Y_{R_{ON}} \right) - \frac{e^{-Y_{R_{1N}}}}{R_{1N}^3} \left(1 + Y_{R_{1N}} \right) \right]. \quad (19)$$

It should be noted that (17), (18), and (19) are identical to Weaver's results.⁶

VERTICAL MAGNETIC DIPOLE (VMD) ANTENNA

The VMD equations can be derived from equations (70), (71), and (72) of an earlier report.⁸ They are

$$E_\phi \sim - \frac{i\omega\mu_0 IA}{4\pi} \sum_{n=0}^{\infty} \rho \epsilon_n \left\{ \frac{e^{-Y_{R_{ON}}}}{R_{ON}^3} \left(1 + Y_{R_{ON}} \right) - \frac{e^{-Y_{R_{1N}}}}{R_{1N}^3} \left(1 + Y_{R_{1N}} \right) \right. \\ \left. + e^{-\gamma a X_2} \left[\frac{1}{A_{1N}^3} - \frac{1}{A_{2N}^3} \right] \right\}, \quad (20)$$

$$H_\rho \sim - \frac{IA}{4\pi} \sum_{n=0}^{\infty} \rho \epsilon_n \left[\frac{X_1}{R_{ON}^5} \left(3 + 3Y_{R_{ON}} + Y_{R_{ON}}^2 \right) e^{-Y_{R_{ON}}} \right. \\ \left. + \frac{3(d + bX_2)}{A_{2N}^5} e^{-\gamma a X_2} \right], \quad (21)$$

and

$$\begin{aligned}
 H_z \sim & -\frac{IA}{4\pi} \sum_{n=0}^{\infty} \epsilon_n \left[\frac{e^{-\gamma R_{ON}}}{R_{ON}^3} \left\{ \left[1 - \frac{3X_1^2}{R_{ON}^2} \right] (1 + \gamma R_{ON}) + \gamma^2 \rho^2 \right\} \right. \\
 & - \frac{e^{-\gamma R_{1N}}}{R_{1N}^3} \left\{ \left[1 - \frac{3X_2^2}{R_{1N}^2} \right] (1 + \gamma R_{1N}) + \gamma^2 \rho^2 \right\} \\
 & \left. + e^{-\gamma a X_2} \left\{ \frac{1}{A_{1N}^3} \left[1 - \frac{3b^2 X_2^2}{A_{1N}^2} \right] - \frac{1}{A_{2N}^3} \left[1 - \frac{3(d - bX_2)^2}{A_{2N}^2} \right] \right\} \right]. \quad (22)
 \end{aligned}$$

DERIVATION OF THE CONDUCTING SLAB FIELD-COMPONENT
EXPRESSIONS FOR THE QUASI-NEAR RANGE

Quasi-near range is defined as the asymptotic part of the quasi-static range, i.e., where the measurement distance (ρ) is much greater than a skin depth in the conducting medium and much greater than the depth of burial of the transmitting and receiving antennas. Generally, ρ must be greater than 3δ and $>3(z+h)$. For the conducting slab case, ρ should also be greater than $3\ell_1$. However, as we shall see later, the requirement that $\rho \geq 2\delta$ and $\rho \geq 2\ell_1$ may be sufficient for most cases.

The quasi-near range approximation is setting the function $u = \sqrt{\lambda^2 + \gamma^2}$ in the exact integral expressions equal to γ , which is the propagation constant in the conducting medium.

LONG HORIZONTAL LINE SOURCE/ANTENNA

For a long horizontal line source antenna, oriented in the x-direction, the electric field within a conducting slab may be written exactly as (for $z > h$)

$$E_X = -\frac{i\omega\mu_0 I}{2\pi} \int_0^{\infty} \frac{F(\lambda)}{u} \cos \lambda y d\lambda, \quad (23)$$

where

$$\frac{F(\lambda)}{u} = \frac{(e^{uh} + R_g e^{-uh})(e^{-uz} + R_g e^{-u(2\ell_1 - z)})}{u(1 - R_g^2 e^{-2u\ell_1})}, \quad (24)$$

$$R_g = \frac{u - u_0}{u + u_0}, \text{ and} \quad (25)$$

$$u_0 = \sqrt{\lambda^2 + \gamma_0^2} \sim \lambda \text{ for the quasi-static range.}$$

The magnetic fields within the conducting slab may be determined from

$$H_Y = -\frac{1}{i\omega\mu_0} \frac{\partial E_X}{\partial z} \text{ and } H_Z = \frac{1}{i\omega\mu_0} \frac{\partial E_X}{\partial y}. \quad (26)$$

Application of the quasi-static ($\gamma_0 \sim 0$) and quasi-near ($u \sim \gamma$) approximations to (24) and (25) results in

$$\frac{F(\lambda)}{u} \sim \frac{2 \left[\cosh \gamma h + \frac{\lambda}{\gamma} \sinh \gamma h \right] \left[\cosh \gamma (\ell_1 - z) + \frac{\lambda}{\gamma} \sinh \gamma (\ell_1 - z) \right]}{\left(\gamma \sinh \gamma \ell_1 \left[1 + \frac{2\lambda}{\gamma} \coth \gamma \ell_1 \right] \right)}. \quad (27)$$

If the slab is not too thin, the denominator of (27) may be approximated as

$$\frac{1}{\gamma \sinh \gamma \ell_1 \left[1 + \frac{2\lambda}{\gamma} \coth \gamma \ell_1 \right]} \sim \frac{1}{\gamma \sinh \gamma \ell_1} \left[1 - \frac{2\lambda}{\gamma} \coth \gamma \ell_1 \right]. \quad (28)$$

Substituting (27) and (28) into (23) and (26), and noting that¹³

$$\int_0^{\infty} \cos \lambda y \, d\lambda = 0 \quad (29)$$

and

$$\int_0^{\infty} \lambda \cos \lambda y \, d\lambda = -\frac{1}{y} \quad (30)$$

results in

$$E_X \sim \left[-\frac{I}{\pi \sigma y^2} \right] \left[Q^2 \right] \left[A(z, h) \right], \quad (31)$$

$$H_Y \sim \left[\frac{I}{\pi \gamma y^2} \right] \left[Q \right] \left[B(z, h) \right], \quad (32)$$

and

$$H_Z \sim \left[\frac{2I}{\pi \gamma y^3} \right] \left[Q^2 \right] \left[A(z, h) \right]. \quad (33)$$

Equations (31), (32), and (33) are each divided into three parts. The first is the quasi-near range field-component expression valid at the surface of a semi-infinite conducting half-space.⁷ The second is the familiar plane-wave correction factor employed to account for the presence of stratification in the earth.¹⁴ For $\sigma_1 \gg \sigma_2$,

$$Q \sim \coth \gamma \ell_1 . \quad (34)$$

The third part accounts for the burial depth of the transmitting and receiving antennas. For the conducting slab situation when z is greater than h ,

$$A(z,h) \sim \frac{2 \cosh \gamma h \cosh \gamma(\ell_1 - z)}{\cosh \gamma \ell_1} - \frac{\sinh \gamma(\ell_1 + h - z)}{\sinh \gamma \ell_1 \coth^2 \gamma \ell_1} \quad (35)$$

and

$$B(z,h) \sim \frac{\cosh \gamma(\ell_1 + h - z)}{\cosh \gamma \ell_1} - \frac{2 \cosh \gamma h \sinh \gamma(\ell_1 - z)}{\sinh \gamma \ell_1} . \quad (36)$$

When h is greater than z , the resulting expressions are

$$A(z,h) \sim \frac{2 \cosh \gamma z \cosh \gamma(\ell_1 - h)}{\cosh \gamma \ell_1} - \frac{\sinh \gamma(\ell_1 + z - h)}{\sinh \gamma \ell_1 \coth^2 \gamma \ell_1} \quad (37)$$

and

$$B(z,h) \sim \frac{2 \sinh \gamma z \cosh \gamma(\ell_1 - h)}{\sinh \gamma \ell_1} - \frac{\cosh \gamma(\ell_1 + z - h)}{\cosh \gamma \ell_1} . \quad (38)$$

It should be noted that

$$\frac{\partial}{\partial z} A(z,h) \sim \frac{\gamma}{Q} B(z,h) \quad (39)$$

and

$$\frac{\partial}{\partial z} B(z,h) \sim \gamma Q A(z,h) . \quad (40)$$

When $z = h = 0$ or ℓ_1 ,

$$A(z,h) \sim 2 - \tanh^2 \gamma \ell_1 \sim 1 \text{ for } |\gamma \ell_1| > 1 \quad (41)$$

and $B(z,h) \sim \pm 1$. Furthermore, when $|\gamma \ell_1| > 2\sqrt{2} (\ell_1/\delta > 2)$ and $\ell_1 > 2(z+h)$,

$$A(z,h) \sim B(z,h) \sim e^{-\gamma(z+h)} . \quad (42)$$

If $h = 0$ and $z = \ell_1$,

$$A(z,h) \sim 2B(z,h) \sim \frac{2}{\cosh \gamma \ell_1}, \quad (43)$$

which is identical to von Aulock's result.¹⁵ (See chapter 4, p. 14 of Kraichman⁷ and Bannister.¹⁶) Furthermore, if $h = 0$ and $\ell_1/\delta > 2$, then

$$A(z,h) \sim 2e^{-\gamma \ell_1} \left[2 \cosh \gamma(\ell_1 - z) - \sinh \gamma(\ell_1 - z) \right] \quad (44)$$

and

$$B(z,h) \sim 2e^{-\gamma \ell_1} \left[\cosh \gamma(\ell_1 - z) - 2 \sinh \gamma(\ell_1 - z) \right], \quad (45)$$

which is identical to von Aulock's result.¹⁵ (Also, see chapter 4, p. 13 in Kraichman.⁷)

HORIZONTAL ELECTRIC DIPOLE (HED) ANTENNA

By following the same procedure outlined in the derivation of the equations for the long horizontal line source antenna, the quasi-near range HED antenna field-component expressions, which are valid within the conducting slab, may readily be determined. They are

$$E_\rho \sim \frac{I\ell \cos \phi}{2\pi\sigma\rho^3} Q^2 A(z,h), \quad (46)$$

$$E_\phi \sim \frac{I\ell \sin \phi}{\pi\sigma\rho^3} Q^2 A(z,h), \quad (47)$$

$$E_z \sim 0, \quad (48)$$

$$H_\rho \sim \frac{I\ell \sin \phi}{\pi\gamma\rho^3} Q B(z,h), \quad (49)$$

$$H_\phi \sim -\frac{I\ell \cos \phi}{2\pi\gamma\rho^3} Q B(z,h), \quad (50)$$

and

$$H_z \sim \frac{3I\ell \sin \phi}{2\pi\gamma\rho^4} Q^2 A(z,h). \quad (51)$$

When $h = 0$ and $z = \ell_1$, the HED antenna expressions reduce to the results previously derived by Bannister.¹⁷

HORIZONTAL MAGNETIC DIPOLE (HMD) ANTENNA

By employing Maxwell's equations and the reciprocity theorem, we see that the quasi-near range HMD antenna field component expressions, which are valid within the conducting slab, may readily be determined from the HED antenna expressions. They are

$$E_{\rho} \sim \frac{i\omega\mu_0 IA \cos \phi}{2\pi\gamma\rho^3} Q B(h,z), \quad (52)$$

$$E_{\phi} \sim \frac{i\omega\mu_0 IA \sin \phi}{\pi\gamma\rho^3} Q B(h,z), \quad (53)$$

$$E_z \sim 0, \quad (54)$$

$$H_{\rho} \sim \frac{IA \sin \phi}{\pi\rho^3} \frac{Q}{\gamma} \frac{\partial B(h,z)}{\partial z}, \quad (55)$$

$$H_{\phi} \sim -\frac{IA \cos \phi}{2\pi\rho^3} \frac{Q}{\gamma} \frac{\partial B(h,z)}{\partial z}, \quad (56)$$

and

$$H_z \sim \frac{3IA \sin \phi}{2\pi\gamma\rho^4} Q B(h,z), \quad (57)$$

where $B(h,z) = B(z,h)$, with h and z interchanged. That is,

$$B(h,z) \sim \frac{\cosh \gamma(\ell_1 + z - h)}{\cosh \gamma\ell_1} - \frac{2 \cosh \gamma z \sinh \gamma(\ell_1 - h)}{\sinh \gamma\ell_1}. \quad (58)$$

Furthermore,

$$\frac{Q}{\gamma} \frac{\partial B(h,z)}{\partial z} \sim \frac{\sinh \gamma(\ell_1 + z - h)}{\sinh \gamma\ell_1} - \frac{2 \sinh \gamma z \sinh \gamma(\ell_1 - h)}{\sinh \gamma\ell_1 \tanh \gamma\ell_1}. \quad (59)$$

VERTICAL MAGNETIC DIPOLE (VMD) ANTENNA

By employing Maxwell's equations and the reciprocity theorem, we see that the quasi-near range VMD antenna field-component expressions, which are

valid within the conducting slab, may easily be determined from the HED antenna expressions. They are

$$E_{\phi} \sim - \frac{3IA}{2\pi\sigma\rho} Q^2 A(h,z) . \quad (60)$$

$$H_{\rho} \sim - \frac{3IA}{2\pi\gamma\rho} Q B(h,z) , \quad (61)$$

and

$$H_z \sim - \frac{9IA}{2\pi\gamma\rho} Q^2 A(h,z) , \quad (62)$$

where $A(h,z) = A(z,h)$, with z and h interchanged. That is,

$$A(h,z) \sim \frac{2 \cosh \gamma z \cosh(\ell_1 - h)}{\cosh \gamma \ell_1} - \frac{\sinh \gamma(\ell_1 + z - h)}{\sinh \gamma \ell_1 \coth^2 \gamma \ell_1} . \quad (63)$$

DISCUSSION

It would be of interest to compare the results derived in this report with some known results. Figures 2 through 6 show comparisons of modified image theory, quasi-near (asymptotic) theory, and Weaver's numerical integration results⁶ for the electric and magnetic fields at the surface ($z = 0$) of a one-skin-depth-thick ($\ell_1 = \delta$) conducting slab produced by an HED located in the middle of the slab ($h/\delta = 0.5$). The normalized amplitude of each component (E' or H') is given by

$$H' = \frac{4\pi\delta^2 H}{I\ell \begin{pmatrix} \sin \phi \\ \cos \phi \end{pmatrix}} \text{ and } E' = \frac{4\pi\sigma\delta^3 E}{I\ell \begin{pmatrix} \sin \phi \\ \cos \phi \end{pmatrix}} . \quad (64)$$

Two values of a and b are considered for the modified image theory plots. The $a = 0.4$ and $b = 0.96$ results should be valid in situations close to the source, and the $a = 0.96$ and $b = 0.4$ results should be valid at further distances. In each of these cases, only five terms of the infinite summation were needed for 1 percent accuracy.

As Weaver has indicated,⁶ this particular model possesses symmetry about the plane $z = h$. When $z = h$, all components that vary as $B(z,h)$ equal zero. Furthermore, if $z = 0$ or ℓ_1 , all components that vary as $A(z,h)$ are equal, whereas all components that vary as $B(z,h)$ are equal and opposite.

Figures 2 and 3 show horizontal electric field comparisons of the modified image theory, asymptotic theory, and numerical integration results. We can see from figure 2 that, for the E_{ρ} component, the modified image theory $a = 0.4$ and $b = 0.96$ curve agrees well with the numerical integration results throughout the range of ρ/δ considered ($0 < \rho/\delta < 3$). However, we observe that beyond approximately 1.25 skin depths, the (simple form) asymptotic theory agrees more closely.

We can see from figure 3 that, for the E_{ϕ} component, the modified image theory $a = 0.4$ and $b = 0.96$ curve agrees well with the numerical integration results for $0 < \rho/\delta < 0.75$, while the $a = 0.96$ and $b = 0.4$ curve more closely agrees for $0.75 < \rho/\delta < 3$. Beyond approximately 2 skin depths, the asymptotic theory provides the better fit to the numerical integration data.

Figures 4, 5, and 6 show the magnetic field comparisons of the modified image theory, asymptotic theory, and numerical integration results. We see from figure 4 that, for the H_{ρ} component, the $a = 0.4$ and $b = 0.96$ curve agrees very closely with the numerical integration results for $\rho/\delta < 0.5$, but only moderately so for $\rho/\delta > 0.5$. The $a = 0.96$ and $b = 0.4$ curve is in good agreement beyond 1.5 skin depths, while the asymptotic theory curve provides the best fit beyond 2.5 skin depths.

In figure 5, we can see that, for the H_{ϕ} component, the modified image theory $a = 0.4$ and $b = 0.96$ curve agrees very closely with the numerical integration results to $\rho/\delta \sim 2$. Beyond that, the asymptotic theory curve provides the best fit.

In figure 6, we can see that, for the H_z component, the modified image theory, $a = 0.4$ and $b = 0.96$ curve agrees very well with the numerical integration results for $\rho/\delta < 1$. Beyond $\rho/\delta = 1$, the $a = 0.96$ and $b = 0.4$ curve agrees more closely. For $\rho/\delta > 2$, the asymptotic theory curve also agrees well with the numerical integration results.

Thus, it appears that the (simple form) asymptotic theory will provide results of sufficient accuracy when the measurement distance is greater than 2 skin depths and greater than twice the slab depth (i.e., $\rho/\delta > 2$ and $\rho/k_1 > 2$).

CONCLUSIONS

Approximate expressions for both the general ac quasi-static and quasi-near fields produced by electric and magnetic dipole antennas located within a conducting slab have been derived by employing finitely conducting earth-image theory techniques and by applying the quasi-near approximation to the basic Sommerfeld integrals.

We have demonstrated that the resultant approximations very closely agree with previously derived numerical integration results. In particular, it appears that the (simple form) asymptotic theory will provide sufficiently accurate results when the measurement distance is greater than 2 skin depths and greater than twice the slab depth.

Although displacement currents in the conducting slab have been ignored in the analysis, they can be included by simply replacing σ with $\sigma + i\omega\epsilon$ in the field strength equations, providing $|\gamma^2| \gg |\gamma_0^2|$. The resultant expressions are applicable to short range electromagnetic propagation in a shallow sea.

It can be seen from Figure 2 that, for the z component, the modified theory agrees very closely with the numerical integration results. In particular, the z component of the magnetic field is shown to be in phase with the electric field, as expected for a lossy medium.

Figure 3 shows the magnitude of the modified theory compared with the numerical integration results. The magnitude of the magnetic field is shown to be in phase with the electric field, as expected for a lossy medium. The results are in good agreement with the numerical integration data.

In Figure 4, we can see that, for the z component, the modified theory agrees very closely with the numerical integration results. In particular, the z component of the magnetic field is shown to be in phase with the electric field, as expected for a lossy medium.

Figure 5 shows the magnitude of the modified theory compared with the numerical integration results. The magnitude of the magnetic field is shown to be in phase with the electric field, as expected for a lossy medium. The results are in good agreement with the numerical integration data.

It is apparent that the modified theory will provide accurate results when the measurement distance is greater than the skin depth. The results are in good agreement with the numerical integration data.

CONCLUSIONS

Approximate expressions for both the general case of a lossy medium and the special case of a lossless medium have been derived. The results are in good agreement with the numerical integration data. The modified theory provides a simple and accurate method for calculating the field strength in a shallow sea.

We have demonstrated that the modified theory provides accurate results when the measurement distance is greater than the skin depth. The results are in good agreement with the numerical integration data.

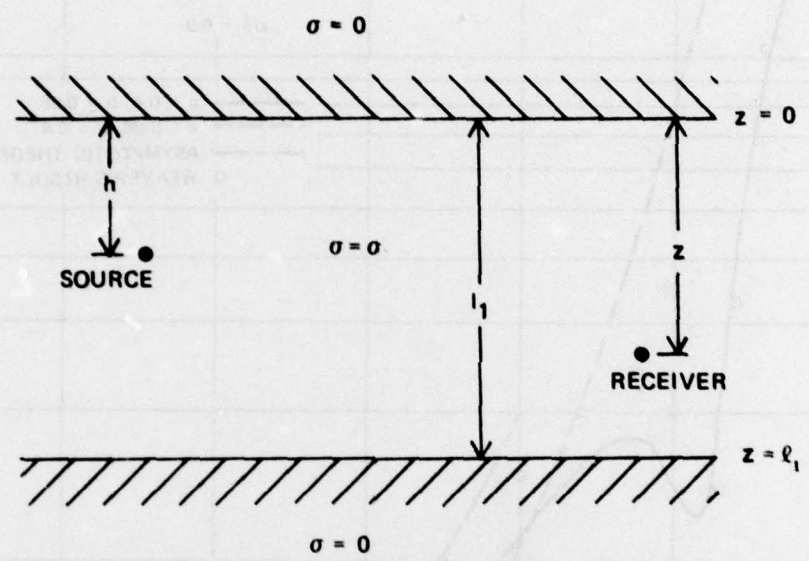


Figure 1. Conducting Slab Geometry

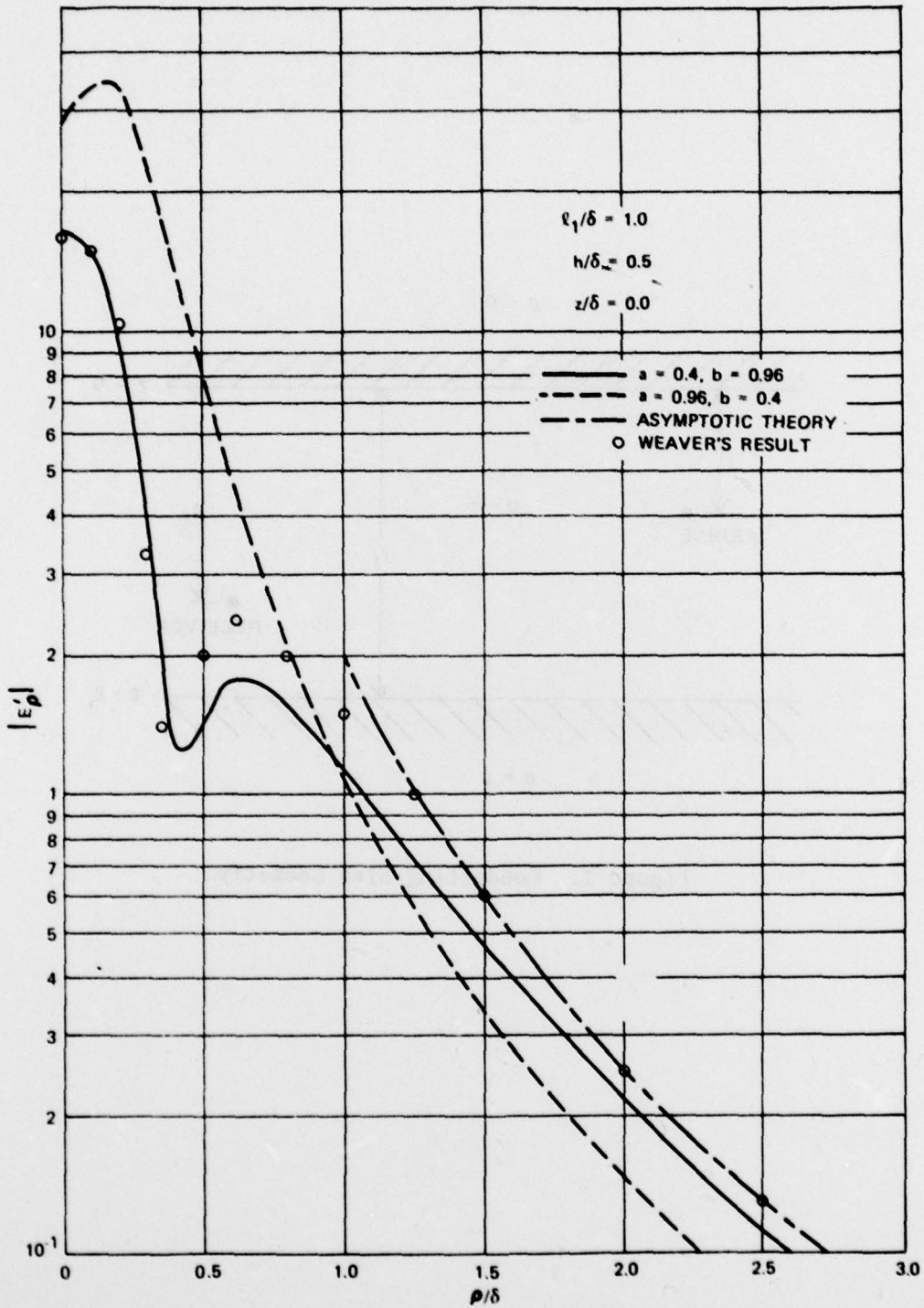


Figure 2. Comparison of Modified Image Theory, Asymptotic Theory, and Weaver's Result for the E'_0 Component

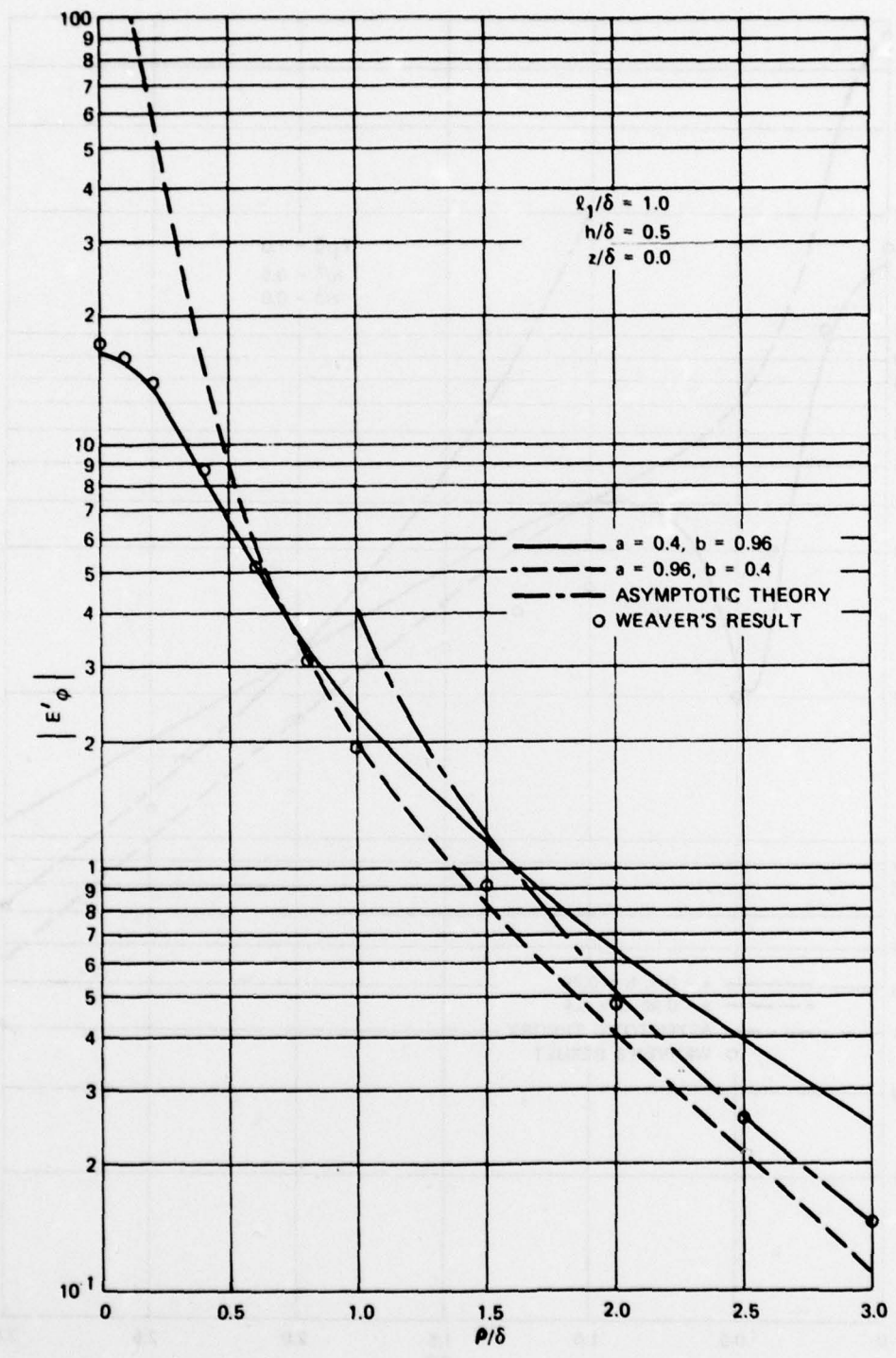


Figure 3. Comparison of Modified Image Theory, Asymptotic Theory, and Weaver's Result for the E'_ϕ Component

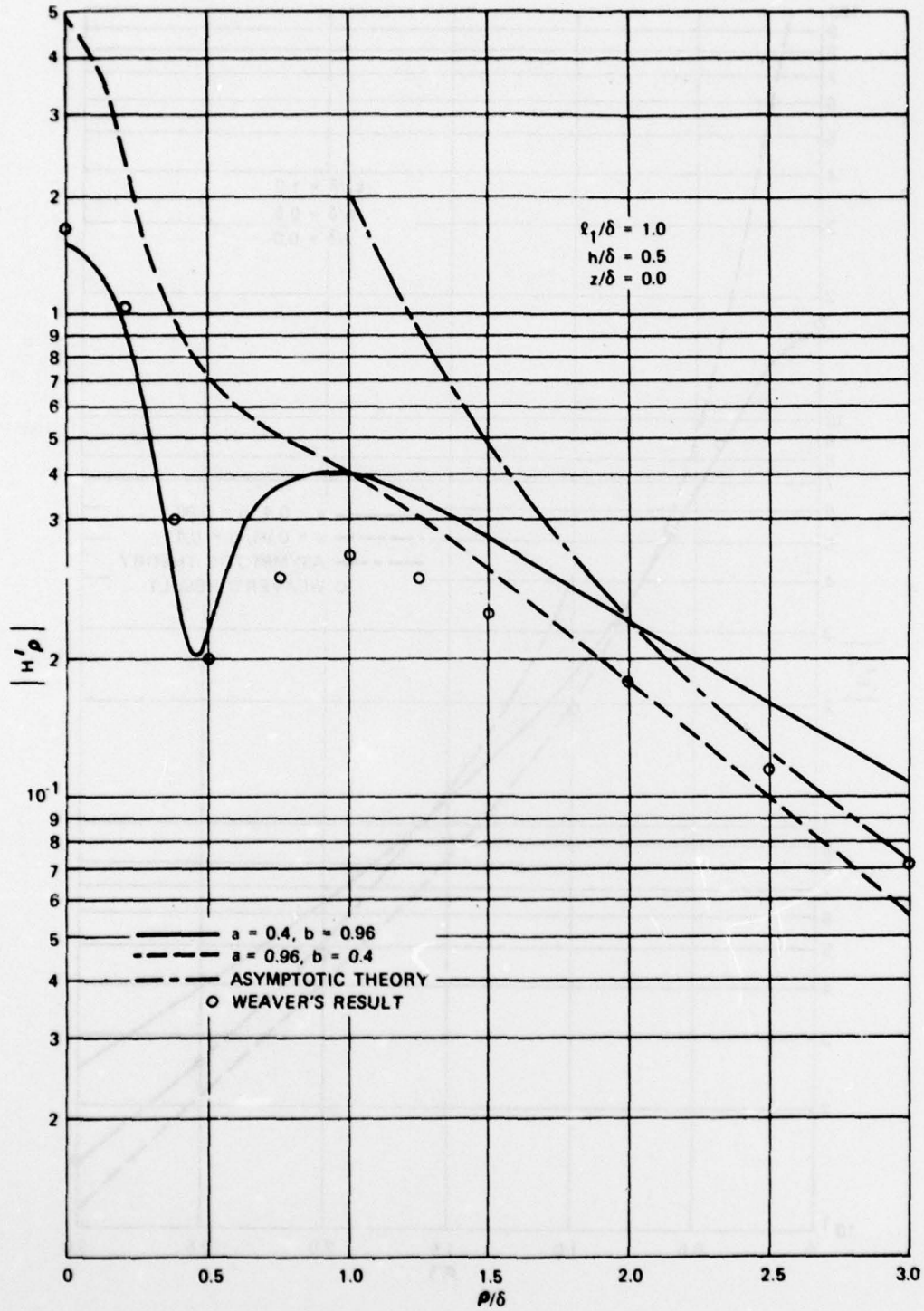


Figure 4. Comparison of Modified Image Theory, Asymptotic Theory, and Weaver's Result for the H_ρ^* Component

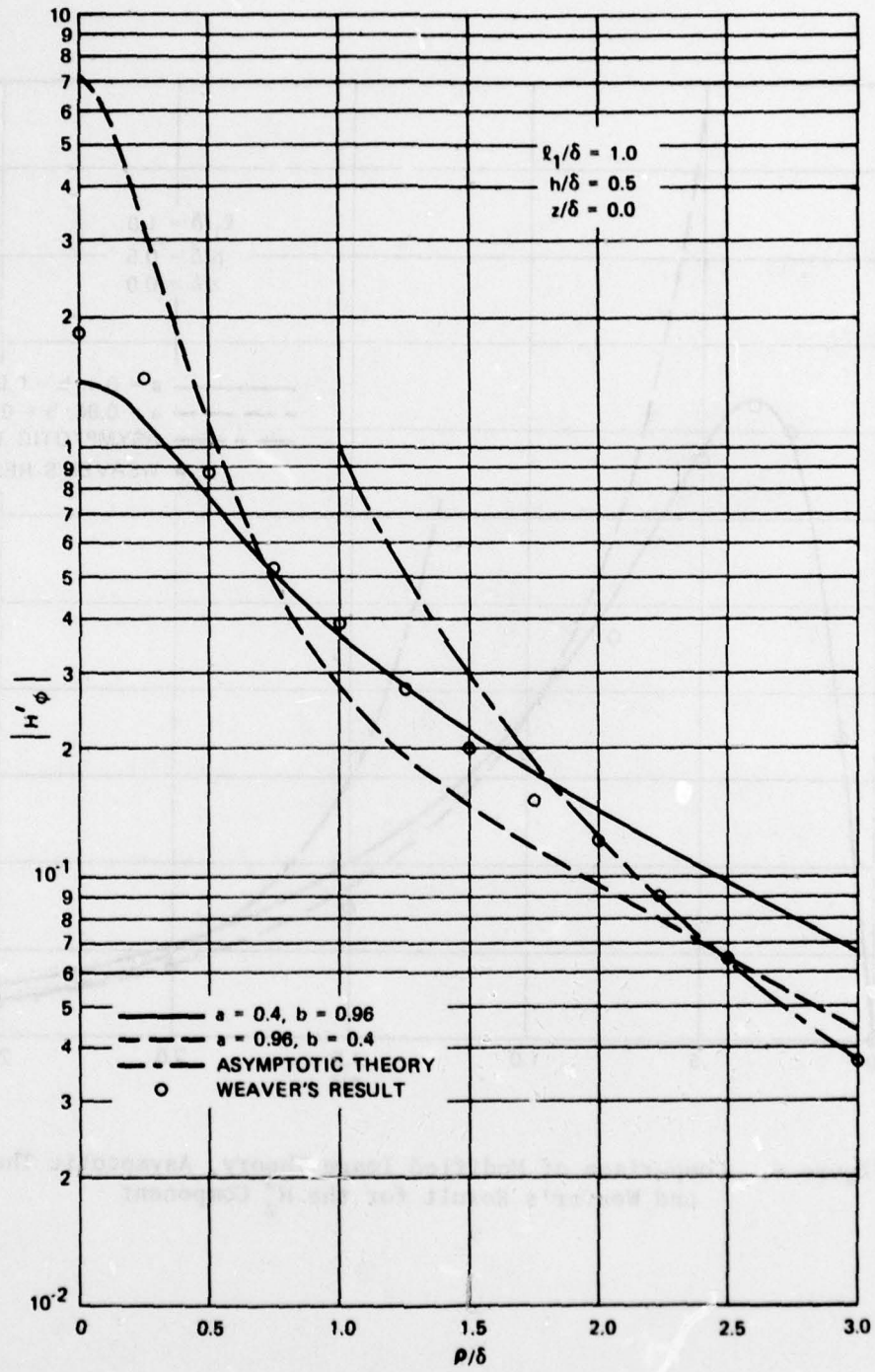


Figure 5. Comparison of Modified Image Theory, Asymptotic Theory, and Weaver's Result for the H'_ϕ Component

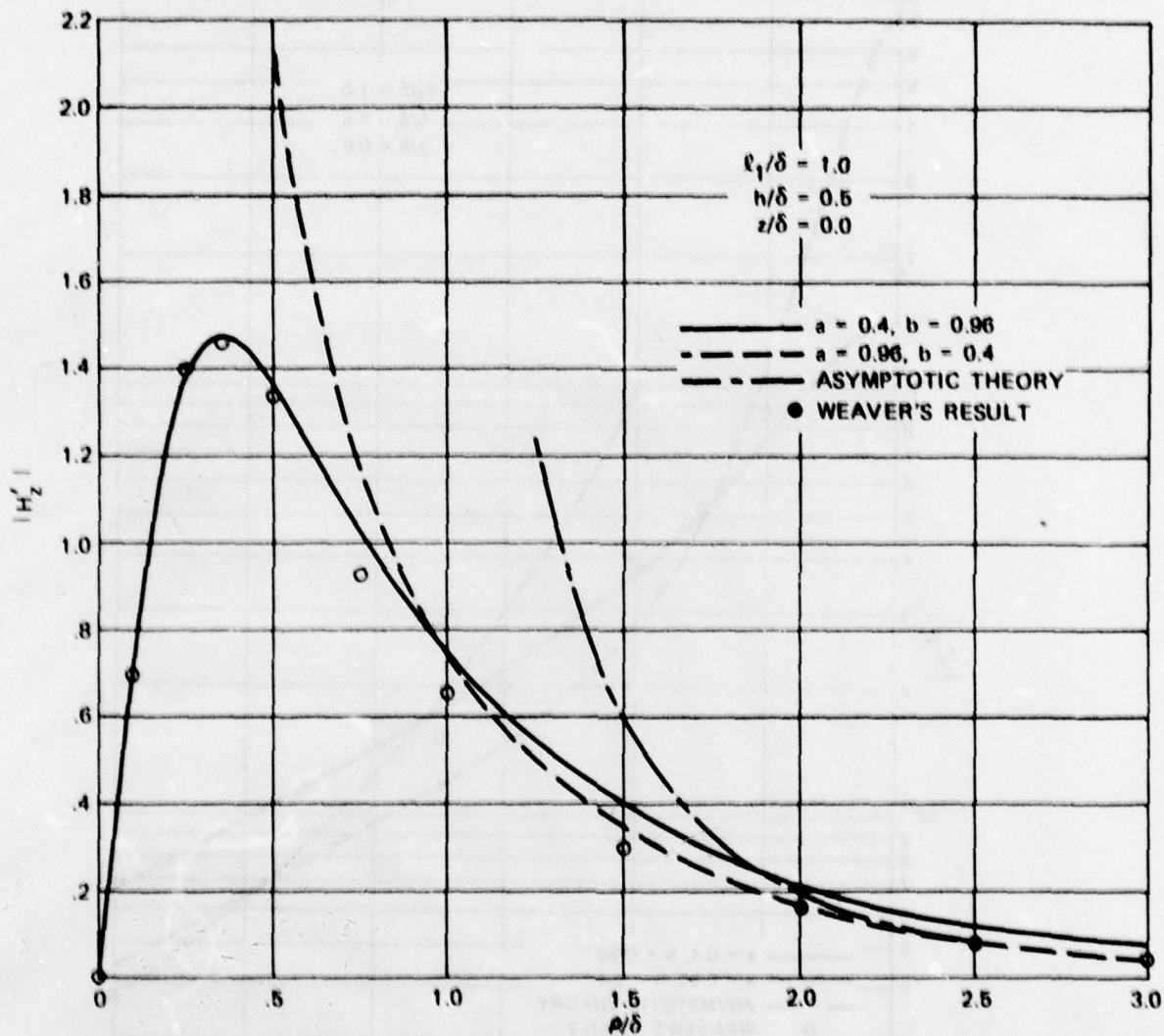


Figure 6. Comparison of Modified Image Theory, Asymptotic Theory, and Weaver's Result for the H_z' Component

REFERENCES

1. J. R. Wait, "The Electromagnetic Fields of a Horizontal Dipole in the Presence of a Conducting Half-Space," Canadian Journal of Physics, vol. 39, 1961, pp. 1017-1028.
2. J. R. Wait and L. L. Campbell, "The Fields of an Electric Dipole in a Semi-Infinite Conducting Medium," Journal of Geophysical Research, vol. 58, 1953, pp. 21-28.
3. J. R. Wait and L. L. Campbell, "The Fields of an Oscillating Magnetic Dipole Immersed in a Semi-Infinite Conducting Medium," Journal of Geophysical Research, vol. 58, no. 2, 1953, pp. 167-178.
4. A. K. Sinha and P. K. Bhattacharya, "Vertical Magnetic Dipole Buried Inside a Homogeneous Earth", Radio Science, vol. 1, no. 3, 1966, pp. 379-395.
5. P. R. Bannister and W. C. Hart, Quasi-Static Fields of Dipole Antennas Below the Earth's Surface, NUSL Technical Report 870, 11 April 1968.
6. J. T. Weaver, "The Quasi-Static Field of an Electric Dipole Embedded in a Two-Layer Conducting Half-Space," Canadian Journal of Physics, vol. 45, 1967, pp. 1981-2002.
7. M. B. Kraichman, Handbook of Electromagnetic Propagation in Conducting Media, U.S. Government Printing Office, Washington, DC, 1970 (second edition, 1976).
8. P. R. Bannister and R. L. Dube, Modified Image Theory Quasi-Static Range Subsurface-to-Subsurface and Subsurface-to-Air Propagation Equations, NUSC Technical Report 5647, Naval Underwater Systems Center, New London, CT, 12 October 1977.
9. P. R. Bannister and R. L. Dube, Numerical Results for Modified Image Theory Quasi-Static Range Subsurface-to-Subsurface and Subsurface-to-Air Propagation, NUSC Technical Report 5775, Naval Underwater System Center, New London, CT, 7 December 1977.
10. J. H. Coggon and H. F. Morrison, "Electromagnetic Investigation of the Sea Floor," Geophysics, vol. 35, no. 3, 1970, pp. 476-489.
11. P. R. Bannister, The Image Theory Quasi-Static Fields of Antennas Above the Earth's Surface, NUSL Technical Report 1061, Naval Underwater System Center, New London, CT, 29 December 1969.

INITIAL DISTRIBUTION LIST

Addressee	No. of Copies
ONR, Code 427, 483, 412-8, 480, 410, Earth Sciences Division (T. Quinn), 463	7
ONR Branch Office, Chicago (F. L. Dowling)	1
NRL, (J. Davis, W. Meyers, R. Dinger, F. Kelly), Code 6451 (D. Forester), 6454 (J. Clement, E. Compy, P. Lubitz, J. Schelleng)	9
NAVELECSYSCOMHQ, Code 03, PME-117, -117-21, -117-213, -117-213A, -117-215	6
NELC, (R. Moler, H. Hughes, R. Pappert, Code 3300)	4
NAVSURFWPNCEN, WR-43 (R. Brown, J. Cunningham, Jr., M. Kraichman)	3
NAVCOASTSYSLAB, Code 721 (C. Stewart), 773 (K. Allen), 792 (M. Wynn, W. Wynn)	4
NAVSEC, Code 6157 B (C. Butler, G. Kahler, D. Muegge)	3
NAVFACENSYSCOM, Code FPO-1C (W. Sherwood), -1C7 (R. McIntyre, A. Sutherland)	3
NAVAIR, Code AIR-0632 B (L. Goertzen)	1
NAVAIRDEVCCEN, Code 2022 (J. Duke, R. Gasser, E. Greeley, A. Ochadlick, L. Ott, W. Payton, W. Schmidt)	7
NAVSHIPYD PTSMH, Code 280 (B. Murdock)	1
AFWTF, Code 01A (CDR W. Danner), 32 (LT R. Elston), 412 (P. Burton, R. Kirkpatrick)	4
NISC, Code 20 (G. Batts), 43 (J. Erdmann), OW17 (M. Koontz)	3
NOSC, Code 407 (C. Ramstedt)	1
NAVPGSCOL, Code 06 (R. Fossum)	1
U.S. Naval Academy, Anna. (C. Schneider)	1
CNO, Code OP-02, 03EG, -090, -23, -902, 941, -942U, 201, -953, -954, -96	11
CNM, Code MAT-00, -03L, -0302, -034, -03T (CAPT Walker), ASW-23	6
SUBASE LANT	1
DDC	12
NAVSUBSUPFACNLON	1
NAVWPNSCEN	1
NAVSUBTRACENPAC	1
CIVENGLAB	1
NAVSUBSCOL	1
NAVWARCOL	1
Engineering Societies Library United Engineering Center 345 East 47th St. New York, NY 10017	1
GTE Sylvania (G. Pucillo, D. Esten, R. Warshawer, D. Boots, R. Row) Needham, MA 02194	5

INITIAL DISTRIBUTION LIST (Cont'd)

Addressee	No. of Copies
Lockheed (J. Reagan, W. Imhof, T. Larsen) Palo Alto, CA 94302	3
Lawrence Livermore Labs (J. Lytle, E. Miller) Livermore, CA	2
Univ. of Nebraska EE Dept. (E. Bahar) Lincoln, NB 68508	1
NOAA (D. Barrick, R. Fitzgerald, D. Grubb, J. Wait (ERL)) U.S. Dept. of Commerce Boulder, CO 80302	4
Newmont Exploration Ltd. (A. Brant) Danbury, CT 06810	1
IITRI (J. Bridges, A. Valentino) Chicago, IL 60068	2
Stanford Univ. Dept. of EE (F. Crawford) Stanford, CA 94305	1
Univ. of Colorado Dept. of EE (D. Chang) Boulder, CO 80302	1
Air Force Cambridge Research Lab (R. Fante) Bedford, MA 01730	1
USGS - Federal Centre Regional Geophysics Branch (F. Frischknecht) Denver, CO 80225	1
Colorado School of Mines Geophysics Dept. (G. Keller) Golden, CO 80401	1

INITIAL DISTRIBUTION LIST (Cont'd)

Addressee	No. of Copies
Univ. of Arizona Dept. of Mining & Geological Engineering (D. Hastings) Tuscon, AZ 85721	1
Univ. of Michigan Radiation Lab (R. Hiatt) Ann Arbor, MI 48105	1
U.S. Army Cold Regions Research & Eng. Lab (P. Hoekstra) Hanover, NH 03755	1
Univ. of Washington Dept. of EE (A. Ishimaru) Seattle, WA 98105	1
Univ. of Wisconsin Dept. of EE (R. King) Madison, WI 53706	1
Univ. of Wyoming Dept. of EE (J. Lindsay, Jr.) Laramie, WY 82070	1
Univ. of Arizona College of Earth Sciences (L. Lepley) Tuscon, AZ 85719	1
Univ. of Illinois Dept. of EE (R. Mittra) Urbana, IL 61801	1
Univ. of Kansas (R. Moore) Lawrence, KS 66044	1
Washington State Univ. Dept. of EE (R. Olsen) Pullman, WA 99163	1
Institute for Telecommunication Services U.S. Dept. of Commerce (R. Ott, D. D. Crombie) Boulder, CO 80302	1
North Carolina State Univ. EE Dept. (R. Rhodes) Raleigh, NC 27607	1

TR 5807

INITIAL DISTRIBUTION LIST (Cont'd)

Addressee	No. of Copies
Ohio State Univ. Dept. of EE (J. Richmond) Columbus, OH 43212	1
MIT Lincoln Laboratory (J. Ruze, D. White, J. Evans, L. Ricardi) Lexington, MA 02137	1
Univ. of Utah Dept. of Geological & Geophysical Sciences (S. Ward) Salt Lake City, UT 84112	1
Purdue Univ. School of EE (W. Weeks) Lafayette, IN 47907	1
Nat'l Oceanographic & Atmospheric Admin. Wave Propagation Lab (G. Little) Boulder, CO 80302	1
Univ. of Pennsylvania Moore School of EE D2 (R. Showers) Philadelphia, PA 19174	
JHU/APL (W. Chambers, P. Gueschel, L. Hart, H. Ko) Silver Spring, MD 20910	4
J. P. Wikswo P.O. Box 12062 Acklen Station Nashville, TN 37212	1
A. C. Fraser-Smith Radioscience Laboratory Durand Bldg., Rm. 205 Stanford University Stanford, CA 94305	1
R. C. Hanson Box 215 Tarzana, CA 91356	1